Aharonov-Bohm effect of excitons in nanorings

Hui Hu,[1] Jia-Lin Zhu,[1,2] Dai-Jun Li,[1] and Jia-Jiong Xiong[1]

[1]*Department of Physics, Tsinghua University, Beijing 100084, People's Republic of China*
[2]*Center for Advanced Study, Tsinghua University, Beijing 100084, People's Republic of China*
(Received 19 October 2000; published 18 April 2001)

The magnetic field effects on excitons in an InAs nanoring are studied theoretically. By numerically diagonalizing the effective-mass Hamiltonian of the problem that can be separated into terms in center-of-mass and relative coordinates, we calculate the low-lying excitonic energy levels and oscillator strengths as a function of the ring width and the strength of an external magnetic field. It is shown that in the presence of Coulomb correlation, the so-called Aharonov-Bohm effect of excitons exists in a finite (but small) width nanoring. However, when the ring width becomes large, the non-simply-connected geometry of nanorings is destroyed, causing the suppression of the Aharonov-Bohm effect. The analytical results are obtained for a narrow-width nanoring in which the radial motion is the fastest one and adiabatically decoupled from the azimuthal motions. The conditional probability distribution calculated for the low-lying excitonic states allows identification of the presence of the Aharonov-Bohm effect. The linear optical susceptibility is also calculated as a function of the magnetic field, to be compared with the future measurements of optical emission experiments on InAs nanorings.

I. INTRODUCTION

Recently, Lorke and collaborators demonstrated the realization of self-assembled InAs nanorings inside a completed field-effect transistor.[1–3] Such small nanorings [with a typical inner (outer) radius of 20 (100) nm and 2–3 nm in height] allow one to study the new non-simply-connected geometry where electrons or holes could propagate coherently (nondiffusively) all throughout.[4–20] In particular, they offer a unique opportunity to explore the so called ''Aharonov-Bohm effect'' (ABE) of an *exciton*, an interesting concept suggested by Chaplik[21] and Römer and Raikh.[22]

Chaplik first predicted the Aharonov-Bohm (AB) oscillation of excitonic levels in *one*-dimensional quantum ring structures,[21] and most recently, Römer and Raikh found similar results with a short-ranged interaction potential by using a quite different analytical approach.[22] In contrast to the general belief that an exciton, being a bound state of electron and hole and thus a *neutral* entity, should not be sensitive to the applied flux, they predicted the possibility of a nonvanishing ABE in one-dimensional rings caused by the *finite* confinement of an exciton. On the other hand, so far the influence of the ring width on ABE has rarely been investigated. Only recently did Song and Ulloa study the magnetic field effect on excitons in a finite width nanoring. They found that the excitons in nanorings behave to a great extent as those in quantum dots of similar dimensions and the finite width of nanorings can suppress completely the ABE predicted for one-dimensional rings.[23] At the moment, however, to what extent the ABE exists in the quasi-one-dimensional (or more important, the *realistic*) nanorings is still unclear and is an open subject for research.

In this paper, we would like to investigate systematically the magnetic field effect on an exciton within a simplified model Hamiltonian, which is applicable to the *realistic* self-assembled semiconducting InAs nanorings.[1–3,24] By diagonalizing the effective-mass Hamiltonian of the problem and calculating the low-lying excitonic energy levels and oscillator strengths as a function of the ring width and the strength of an external magnetic field, we show an evident ABE for nanorings with a finite but small ring width. The numerical results are well interpreted with the analytical results for a narrow-width nanoring in which the radial motion is the fastest one and adiabatically decoupled from the azimuthal motions, and also well understood by the conditional probability distribution calculated for the low-lying excitonic states. The following is a summary of our main results:

(i) In the presence of a Coulomb interaction between the electron and hole, there is *no* ABE for the *ground excitonic state* for *all* the ring widths due to the intrinsic divergence of the ground-state energy of one-dimensional excitons.

(ii) Some of the low-lying excited excitonic energy levels and oscillator strengths can show a periodic, Aharonov-Bohm-type oscillation, as a function of the magnetic field. The periodicity of oscillations is equal to $\Phi_0 \equiv h/e$—the universal flux quantum.

(iii) In addition to the overall blueshifts caused by the diamagnetic effect, the linear optical susceptibility traces apparently show ABE oscillations with the magnetic field for some of excited states.

The remainder of this paper is organized as follows. In Sec. II, we present the model Hamiltonian for a nanoring and the solution method. As a first approximation, the nanoring structure is modeled by a ringlike confinement potential in which we can separate the Hamiltonian into terms in center-of-mass and relative coordinates. Subsequently (Sec. III), we give the analytical results for the narrow-width nanorings with $m_e^* = m_h^*$. By calculating the tunneling possibility for three typical electron-hole interaction potential $V_{e\text{-}h}(\varphi)$, we explore the underlying physics of ABE, and the main results of Chaplik and of Römer and Raikh are recovered. Section IV is devoted to the detailed discussion of numerical results for different ring widths and magnetic fields, including the low-lying energy levels, oscillator strengths, conditional

probability distributions, pair-correlation functions, and the linear optical susceptibility. Finally, we summarize our results in Sec. V.

II. MODEL AND NUMERICAL METHOD

We start from a simplified model Hamiltonian for a two-dimensional exciton in an InAs nanoring and in a static magnetic field, simulating recent experimental nanoring structures.[1–3,24] The exciton is described by an electron-hole pair ($i = e, h$) with an effective band edge mass m_i^* moving in the x-y plane. The ringlike structure is well described by the potential, $U(\mathbf{r}_i) = (1/2R_0^2) m_i^* \omega_i^2 (\mathbf{r}_i^2 - R_0^2)^2$, which reproduces a soft barrier $m_i^* \omega_i^2 R_0^2/2$ at the center of the sample produced by self-assembly.[1–3,24] Here, R_0 is the radius of the ring and ω_i is the characteristic frequency of the radial confinement, giving a characteristic ring width $W \approx \sqrt{2\hbar/m_i^* \omega_i}$ for each particle. The whole system is subjected to an external magnetic field perpendicular to the x-y plane. The resulting model Hamiltonian is thus given by

$$\mathcal{H} = \sum_{i=e,h} \left[\frac{[\mathbf{p}_i - q_i \mathbf{A}(\mathbf{r}_i)]^2}{2m_i^*} + U(\mathbf{r}_i) \right] - \frac{e^2}{4\pi\varepsilon_0 \varepsilon_r |\mathbf{r}_e - \mathbf{r}_h|}, \tag{1}$$

where $\mathbf{r}_i = (x_i, y_i)$ and $\mathbf{p}_i = -i\hbar \nabla_i$ denote the position vector and momentum operator, ε_0 is the vacuum permittivity, and ε_r is the static dielectric constant of the host semiconductor. $q_e = -e$ and $q_h = +e$. We use symmetric gauge to introduce the external magnetic field, i.e., $\mathbf{A}(\mathbf{r}_e) = \frac{1}{2}\mathbf{B} \times (\mathbf{r}_e - \mathbf{r}_h)$ and $\mathbf{A}(\mathbf{r}_h) = -\frac{1}{2}\mathbf{B} \times (\mathbf{r}_e - \mathbf{r}_h)$.

It should be pointed out that the present ringlike confinement potential can be rewritten as $U(\mathbf{r}_i) = \frac{1}{2}m_i^* \omega_i^2 (r_i - R_0)^2 (r_i + R_0)^2/R_0^2$. If one replaces the operator r_i in factor $(r_i + R_0)^2/R_0^2$ by its mean value $\langle r_i \rangle = R_0$, the confinement potential returns to the widely used parabolic form.[3,5,6,10,17,19,23] On the other hand, in the limit of the small radius R_0 or for a small potential strength ω_i, the soft barrier at the ring center is very weak, and the description of the nanoring is closer to that of a quantum dot. For a fixed ring width (or potential strength), the crossover from nanorings to quantum dots is determined by $R_0 \sim (\sqrt{2}/2)W$ or $\hbar\omega_i/2 \sim m_i^* \omega_i^2 R_0^2/2$, which means the lowest energy of radial confinement is comparable to the soft barrier at the ring center. It should also be pointed out that our ringlike confinement potential has been used to calculate the far-infrared spectroscopy for a two-electron nanoring,[25] in good agreement with the recent experiment done by Lorke *et al.*[3] In Fig. 1, we show the schematic geometry of InAs nanorings with radius $R_0 = 20$ nm for electrons. Figures 1(a) and 1(b) correspond to two different ring widths $W = 10$ and 7 nm, respectively.

In terms of the relative coordinate $\mathbf{r} = \mathbf{r}_e - \mathbf{r}_h$ and center-of-mass coordinate $\mathbf{R} = (m_e^* \mathbf{r}_e + m_h^* \mathbf{r}_h)/(m_e^* + m_h^*)$ the model Hamiltonian can be separated into the motion of center of mass, relative motion of the electron-hole pair, and the mixed part:

$$\mathcal{H} = \mathcal{H}_{cm}(\mathbf{R}) + \mathcal{H}_{rel}(\mathbf{r}) + \mathcal{H}_{mix}(\mathbf{R},\mathbf{r}),$$
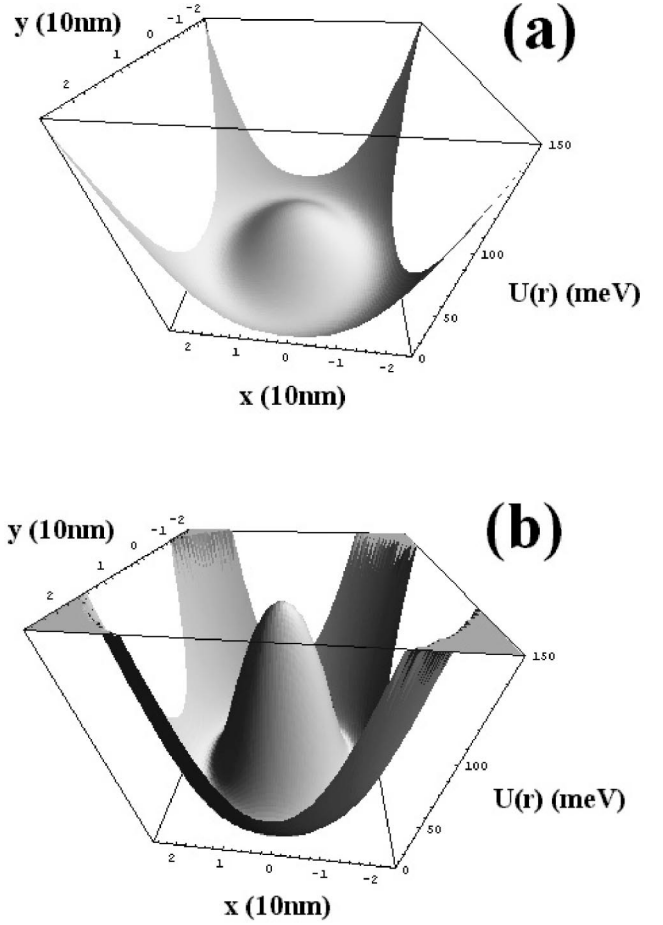

FIG. 1. Schematic geometry of InAs nanorings with radius $R_0 = 20$ nm and width (a) $W = 10$ nm or (b) 7 nm for electrons. $m_e^* = 0.067 m_e$.

$$\mathcal{H}_{cm}(\mathbf{R}) = \frac{\mathbf{P}_{cm}^2}{2M} + \frac{1}{2} M \omega_{cm}^2 \frac{(\mathbf{R}^2 - R_0^2)^2}{R_0^2},$$

$$(2)$$

$$\mathcal{H}_{rel}(\mathbf{r}) = \frac{\mathbf{p}_{rel}^2}{2\mu} + \frac{e^2 B^2}{8\mu} r^2 + \frac{eB}{2} \left(\frac{1}{m_e^*} - \frac{1}{m_h^*} \right) \mathbf{r}$$
$$\times \mathbf{p}_{rel} + \frac{\mu}{2} \frac{(m_h^{*3} \omega_e^2 + m_e^{*3} \omega_h^2)}{M^3} \frac{r^4}{R_0^2}$$
$$- \mu \omega_{rel}^2 r^2 - \frac{e^2}{4\pi\varepsilon_0 \varepsilon_r r},$$

$$\mathcal{H}_{mix}(\mathbf{R},\mathbf{r}) = \frac{eB}{M} \mathbf{r} \times \mathbf{P}_{cm} - 2\mu(\omega_e^2 - \omega_h^2) \left(\mathbf{R} \cdot \mathbf{r} - \frac{\mathbf{R}^3 \cdot \mathbf{r}}{R_0^2} \right)$$
$$+ \mu \omega_{rel}^2 \frac{[R^2 r^2 + 2(\mathbf{R} \cdot \mathbf{r})^2]}{R_0^2}$$
$$+ 2\mu \frac{(m_h^{*2} \omega_e^2 - m_e^{*2} \omega_h^2)}{M^2} \frac{\mathbf{R} \cdot \mathbf{r}^3}{R_0^2},$$

where $\mu = m_e^* m_h^*/M$ is the electron-hole reduced mass and $M = m_e^* + m_h^*$ is the total mass. We have also introduced a center-of-mass frequency $\omega_{cm} = \sqrt{(m_e^* \omega_e^2 + m_h^* \omega_h^2)/M}$ and a relative frequency $\omega_{rel} = \sqrt{(m_h^* \omega_e^2 + m_e^* \omega_h^2)/M}$.

The main purpose in the change of variable above is to use the solutions of H_{cm} and H_{rel} as a basis for solving the full Hamiltonian. Those solutions, i.e., labeled by $\psi_\lambda^{cm}(\mathbf{R})$ and $\psi_{\lambda'}^{rel}(\mathbf{r})$, can be solved by the series expansion method.[26,27] Here, $\lambda = \{n_{cm}, l_{cm}\}$ and $\lambda' = \{n_{rel}, l_{rel}\}$ represent the quantum number pair of the radial quantum number n and orbital angular-momentum quantum number l. Another advantage of the separation of center-of-mass and relative coordinates is that the negative Coulomb interaction $-e^2/4\pi\varepsilon_0\varepsilon_r r$ appears in H_{rel} only, and the well-known poor convergence of the parabolic basis is thus avoided when the characteristic scale of systems is beyond the effective Bohr radius.[23,28] We now search for the wave functions of the exciton in the form

$$\Psi = \sum_{\lambda,\lambda'} A_{\lambda,\lambda'} \psi_\lambda^{cm}(\mathbf{R}) \psi_{\lambda'}^{rel}(\mathbf{r}). \quad (3)$$

Due to the cylindrical symmetry of the problem, the exciton wave functions can be labeled by the total orbital angular momentum $L = l_{cm} + l_{rel}$. To obtain the coefficients $A_{\lambda,\lambda'}$, the total Hamiltonian is diagonalized in the space spanned by the product states $\psi_\lambda^{cm}(\mathbf{R})\psi_{\lambda'}^{rel}(\mathbf{r})$. In the present calculations, we first solve the single-particle problem of center-of-mass and relative Hamiltonians H_{cm} and H_{rel}, keep several hundreds of the single-particle states, and then pick up the low-lying energy levels to construct several thousands of product states. Note that our numerical diagonalization scheme is very efficient and essentially exact in the sense that the accuracy can be improved as required by increasing the total number of selected product states.

Once the coefficients $A_{\lambda,\lambda'}$ are obtained, one can calculate directly the measurable properties, such as the linear optical susceptibility of the nanorings, whose imaginary part is related to the absorption intensity measured by optical emission experiments. In theory, the linear optical susceptibility is proportional to the dipole matrix elements between one electron-hole pair j state and the vacuum state, which in turn is proportional to the oscillator strengths F_j. In the dipole approximation, it is given by[28–30]

$$F_j = \left| \int \int d\mathbf{R}\, d\mathbf{r}\, \Psi(\mathbf{R}, \mathbf{r}) \delta(\mathbf{r}) \right|^2$$
$$= \left| \sum_{\lambda,\lambda'} A_{\lambda,\lambda'} \psi_{\lambda'}^{rel}(\mathbf{0}) \int d\mathbf{R}\, \psi_\lambda^{cm}(\mathbf{R}) \right|^2, \quad (4)$$

where the factor $\psi_{\lambda'}^{rel}(\mathbf{0})$ and the integral over $\mathbf{R}$ ensure that only the excitons with $L = 0$ are created by absorbing photons. Therefore, the frequency dependence of the linear optical susceptibility $\chi(\omega)$ can be expressed as[28–30]

$$\chi(\omega) \propto \sum_j \frac{F_j}{\hbar\omega - E_g - E_j - i\Gamma}, \quad (5)$$

where E_g and E_j are the respective semiconducting band gap of InAs and energy levels of the exciton, and Γ has been introduced as a phenomenological broadening parameter.

III. NARROW-WIDTH NANORINGS

In order to explore the underlying physics of ABE, we first consider a narrow-width nanoring in which the analytical results are variable. We restrict ourselves with the condition $m_e^* = m_h^* = m^*$, but the general properties of nanorings are not affected by this constraint. The technique employed in this section follows directly the previous works of Wendler, Fomin, and Chaplik describing the rotating Wigner molecule behavior in quantum rings.[14–16,31]

By introducing polar coordinates in the x-y plane $\mathbf{r}_i = (r_i, \varphi_i)$, the relative azimuthal coordinate $\varphi = \varphi_e - \varphi_h$, and the azimuthal coordinate $\Theta = (\varphi_e + \varphi_h)/2$ that describes the motion of the electron-hole pair as a whole, the Hamiltonian (1) reads

$$\mathcal{H} = \sum_{i=e,h} \left\{ \left[-\frac{\hbar^2}{2m^*} \left(\frac{\partial^2}{\partial r_i^2} + \frac{1}{r_i} \frac{\partial}{\partial r_i} \right) + U(r_i) \right] \right\}$$
$$- \frac{\hbar^2}{2m^*} \left\{ \frac{1}{r_e^2} \left(\frac{\partial}{\partial\varphi} - i\frac{\Phi_e}{\Phi_0} \right)^2 + \frac{1}{r_h^2} \left(\frac{\partial}{\partial\varphi} - i\frac{\Phi_h}{\Phi_0} \right)^2 \right.$$
$$+ \left(\frac{1}{r_e^2} + \frac{1}{r_h^2} \right) \frac{1}{4} \frac{\partial^2}{\partial\Theta^2} + \left(\frac{1}{r_e^2} - \frac{1}{r_h^2} \right) \frac{\partial}{\partial\varphi} \frac{\partial}{\partial\Theta} \right\}$$
$$+ V_{e\text{-}h}(|\mathbf{r}_e - \mathbf{r}_h|), \quad (6)$$

where $\Phi_e = \pi B r_e^2$ and $\Phi_h = \pi B r_h^2$. For a narrow-width nanoring, i.e., $W \ll R_0$, the radial motion is much faster than the azimuthal motions. Hence the radial motion is *adiabatically decoupled* from the azimuthal motions with the result

$$\Psi(r_e, r_h; \varphi, \Theta) = \sum_{n_e, n_h} \Xi_{n_e, n_h}(r_e, r_h) \psi_{n_e, n_h}(\varphi, \Theta) \quad (7)$$

for the excitonic states. $\Xi_{n_e, n_h}(r_e, r_h)$ is a product of the corresponding single-particle wave functions $\chi_{n_i}(r_i)$ with eigenenergies $\varepsilon_{n_i}^{rad}$ ($n_i = 0,1,2,\ldots$), which describe the radial motion of electrons or holes with zero angular momentum. Because the single-particle wave functions are orthonormalized, the set $\{\Xi_{n_e, n_h}(r_e, r_h)\}$ forms a closure set of orthonormalized functions. The azimuthal wave function should satisfy the *single-valuedness boundary conditions*, i.e., $\psi_{n_e, n_h}(\varphi_e, \varphi_h) = \psi_{n_e, n_h}(\varphi_e + 2\pi, \varphi_h) = \psi_{n_e, n_h}(\varphi_e, \varphi_h + 2\pi) = \psi_{n_e, n_h}(\varphi_e + 2\pi, \varphi_h + 2\pi)$, or in terms of the new variables φ and Θ, $\psi_{n_e, n_h}(\varphi, \Theta) = \psi_{n_e, n_h}(\varphi + 2\pi, \Theta + \pi) = \psi_{n_e, n_h}(\varphi, \Theta + 2\pi)$.

As long as the above-stated criterion of the adiabatic approximation is satisfied, the excited states of radial motion lie high above the ground state. As a consequence we can restrict the consideration to the ground state of the radial motion because here only the lowest-lying states are of interest. Thus we take only $n_e = n_h = 0$ and substitute Eq. (7)

into the Schrödinger equation $\mathcal{H}\Psi = E\Psi$, multiply both parts by $\Xi_{0,0}(r_e, r_h)$, and integrate over r_e, r_h. Hence the variables φ and Θ become separated:

$$\left\{ -\frac{\hbar^2}{m^*}\left\langle\frac{1}{r_e^2}\right\rangle\left[\left(\frac{\partial}{\partial\varphi} - i\frac{\Phi}{\Phi_0}\right)^2 + \frac{1}{4}\frac{\partial^2}{\partial\Theta^2}\right]\right.$$

$$+ \left\langle V_{e-h}\left(\sqrt{r_e^2 + r_h^2 - 2r_e r_h\cos\varphi}\right)\right\rangle$$

$$\left. + 2\varepsilon_0^{rad} - E\right\}\psi_{0,0}(\varphi,\Theta) = 0, \qquad (8)$$

where $\Phi = \langle\Phi_e\rangle = \langle\Phi_h\rangle$ in the first-order approximation, and $\langle\ \rangle$ denotes the average with the radial wave functions

$$\langle\cdots\rangle = \int dr_e r_e \int dr_h r_h \Xi_{0,0}^*(r_e, r_h)\cdots\Xi_{0,0}(r_e, r_h). \quad (9)$$

The magnetic flux in Eq. (8) can be removed by a gauge transformation with the price of introducing the *twisted boundary conditions*:

$$\psi_{0,0}(\varphi,\Theta) = e^{i2\pi\Phi/\Phi_0}\psi_{0,0}(\varphi + 2\pi, \Theta + \pi),$$

$$\psi_{0,0}(\varphi,\Theta) = \psi_{0,0}(\varphi,\Theta + 2\pi). \qquad (10)$$

It is obvious from Eq. (8) that the relative azimuthal motion is decoupled from the azimuthal motion of the electron-hole pair as a whole. Therefore the azimuthal wave function can be represented in the form

$$\psi_{0,0}(\varphi,\Theta) = \Phi_j^p(\varphi)Q_\nu(\Theta), \qquad (11)$$

where

$$Q_\nu(\Theta) = \frac{1}{\sqrt{2\pi}}e^{i\nu\Theta}, \qquad (12)$$

and $\Phi_j^p(\varphi)$ is a solution of the equation

$$\left\{-\frac{\hbar^2}{m^*R_0^2}\frac{\partial^2}{\partial\varphi^2} + V_{e-h}\left(2R_0\left|\sin\frac{\varphi}{2}\right|\right) - \varepsilon_j^{r.a.,p}\right\}\Phi_j^p(\varphi) = 0. \qquad (13)$$

Here we have used

$$\left\langle\frac{1}{r_e^2}\right\rangle = \frac{1}{R_0^2},$$

$$\left\langle V_{e-h}\left(\sqrt{r_e^2 + r_h^2 - 2r_e r_h\cos\varphi}\right)\right\rangle = V_{e-h}\left(2R_0\left|\sin\frac{\varphi}{2}\right|\right).$$

The index p describes the possible symmetry types of $\Phi_j^p(\varphi)$ and can be specified below by the twisted boundary condition. In Fig. 2, we show three typical types of electron-hole interaction potentials $V_{e-h}(2R_0|\sin(\varphi/2)|)$ with 2π periodicity. In the view of the excitonic state, the potential should be strong enough to bind the electron-hole pair, and then the relative azimuthal motion is strongly localized in each potential well. Thus the relative azimuthal wave function can be considered in the tight-binding-like form
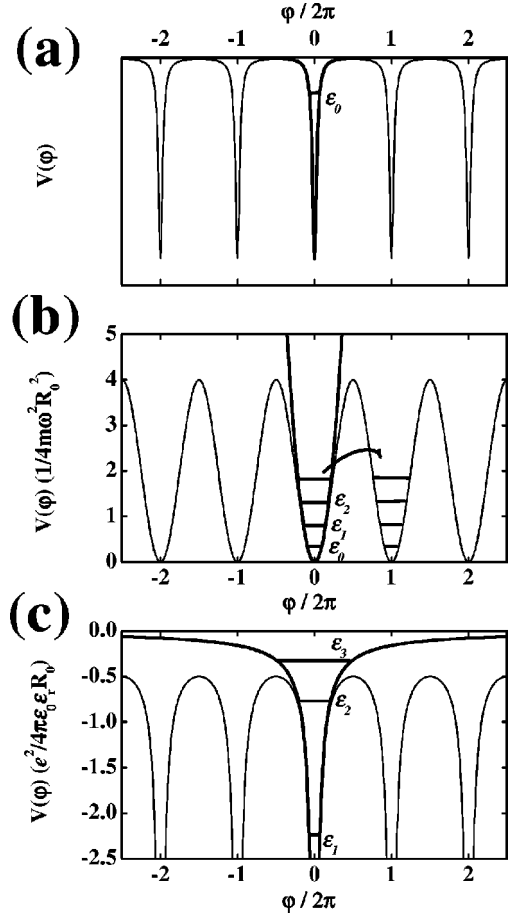

FIG. 2. Scheme of different interaction potentials $V_{e-h}(\varphi)$ as a function of the relative azimuthal coordinate $\varphi = \varphi_e - \varphi_h$. (a) Short-ranged form $-2\pi V_0\delta(2\sin(\varphi/2))$, (b) parabolic form $(m^*\omega^2\rho^2/4)[2\sin(\varphi/2)]^2$, and (c) Coulomb form $-e^2/4\pi\varepsilon_0\varepsilon_r\rho|2\sin(\varphi/2)|$. The potential of a given single well with minimum at $\varphi = 0$, $V_{e-h}^{SW,0}(\varphi)$ is delineated by the thick solid line. Some low-lying energy levels for each well are also indicated.

$$\Phi_j^p(\varphi) = \sum_{Q=-\infty}^{+\infty}\exp(ip\varphi_Q)\phi_j(\varphi - \varphi_Q), \qquad (14)$$

where $\varphi_Q = 2\pi Q; Q = 0, \pm 1, \pm 2, \ldots$. The wave function $\phi_j(\varphi - \varphi_Q)$ of a single well satisfies the equation

$$\left\{-\frac{\hbar^2}{m^*R_0^2}\frac{\partial^2}{\partial\varphi^2} + V_{e-h}^{SW,Q}(\varphi) - \varepsilon_j^{r.a.}\right\}\phi_j(\varphi - \varphi_Q) = 0, \qquad (15)$$

where $V_{e-h}^{SW,Q}(\varphi)$ is the potential of a given single well with minimum at $\varphi = \varphi_Q$, which coincides with the periodic potential $V_{e-h}(2R_0|\sin(\varphi/2)|)$ in the region $|\varphi - \varphi_Q| < \pi$. Note that the tight-binding-like relative azimuthal wave function satisfies the Floquet-Bloch theorem, which is applicable to the periodic potential.

Combining Eqs. (12), (14), and (11) and substituting them into the twist boundary condition, Eq. (10), we obtain

$$\nu = \text{integer}, \qquad (16)$$

$$p + \frac{\nu}{2} + \frac{\Phi}{\Phi_0} = \text{integer}.$$

It becomes obvious that ν describes the total angular momentum of excitons.

The tunneling through the potential from well to well leads to an explicit dependence of the energy levels $\varepsilon_j^{r.a.,p}$ on the symmetry parameter p and thus results in *energy bands* as a function of the magnetic flux Φ. In the tight-binding approximation, it is given by

$$\varepsilon_j^{r.a.,p} = \varepsilon_j^{r.a.} - t_{0,j} - 2t_{1,j} \cos\left(2\pi \frac{\Phi}{\Phi_0} + \pi\nu \right), \quad (17)$$

where

$$t_{0,j} = -\int d\varphi\, \phi_j(\varphi)[V_{e-h}(\varphi) - V_{e-h}^{SW,0}(\varphi)]\phi_j(\varphi),$$

$$t_{1,j} = -\int d\varphi\, \phi_j(\varphi)[V_{e-h}(\varphi) - V_{e-h}^{SW,0}(\varphi)]\phi_j(\varphi - \varphi_1). \quad (18)$$

It is obvious from Eq. (17) that the hopping integral $t_{1,j}$ determines the width of the energy band $\varepsilon_j^{r.a.,p}$ and causes the Aharonov-Bohm-like oscillation in energy levels. However, as follows from the detailed discussion of this effect, $t_{1,j}$ is typically exponentially small compared with $\varepsilon_j^{r.a.,p}$. Only when $\varepsilon_j^{r.a.}$ is close to the maximum of interaction potential $V_{e-h}(\pi)$ does $t_{1,j}$ have a finite value. In other words, in order to access the measurable AB effect, the bound electron and hole should have a possibility to tunnel in the opposite directions and meet each other "on the opposite side of the nanoring" ($\varphi = \pi$).

Using the wave function (11) of a state with a fixed angular momentum ν, we finally obtain the eigenenergies of the full Hamiltonian,

$$E_{0,0,p,j,\nu} = 2\varepsilon_0^{rad} + \varepsilon_j^{r.a.,p} + \frac{\hbar^2\nu^2}{4m^*R_0^2}, \quad (19)$$

and the expression for the oscillation strengths

$$F_j = \frac{|\Phi_j^p(0)|^2}{\int_{-\pi}^{+\pi} d\varphi |\Phi_j^p(\varphi)|^2} \delta_{\nu,0}. \quad (20)$$

In the following we consider the detailed examples for three typical electron-hole interaction potentials, restricting ourselves with $\nu = 0$.

A. Short-ranged potential

We use the δ potential to simulate the short-ranged potential, i.e., $V_{e-h}(2R_0|\sin(\varphi/2)|) = -2\pi V_0 \delta(2|\sin(\varphi/2)|)$, and choose $V_{e-h}^{SW,Q}(\varphi) = -2\pi V_0 \delta(\varphi - \varphi_Q)$ [see Fig. 2(a)]. By solving the one-dimensional Schrödinger equation

$$\left\{ -\frac{\hbar^2}{m^*R_0^2} \frac{\partial^2}{\partial\varphi^2} - 2\pi V_0 \delta(\varphi - \varphi_Q) - \varepsilon_j^{r.a.} \right\} \phi_j(\varphi - \varphi_Q) = 0,$$

we obtain one bound eigenstate with the eigenfunction and eigenvalue

$$\phi_0(\varphi - \varphi_Q) = \sqrt{k} \exp(-k|\varphi - \varphi_Q|), \quad (21)$$

$$\varepsilon_0^{r.a.} = -\frac{\hbar^2 k^2}{m^*R_0^2} = -\pi V_0 k, \quad (22)$$

respectively. Here $k \equiv \pi V_0 / (\hbar^2/m^*R_0^2) \gg 1$. Substituting the single-well wave function (21) in Eq. (18), in the limit of large k, we get the result

$$t_{0,j} \approx 4\pi V_0 k \exp(-4\pi k),$$

$$t_{1,j} \approx 2\pi V_0 k \exp(-2\pi k),$$

and

$$\varepsilon_0^{r.a.,p} \approx -\pi V_0 k \left[1 + 4 \cos\left(\frac{2\pi\Phi}{\Phi_0} \right) \exp(-2\pi k) \right]. \quad (23)$$

Note that the expression for $\varepsilon_0^{r.a.,p}$ agrees exactly with that obtained by Römer and Raikh [Eq. (19) in Ref. 22].

B. Harmonic potential

In this case the electron-hole interaction potential and single-well potential are given by

$$V_{e-h}\left(2R_0 \left| \sin\frac{\varphi}{2} \right| \right) = \frac{m^*R_0^2}{4} \omega^2 \left(2\sin\frac{\varphi}{2} \right)^2,$$

$$V_{e-h}^{SW,Q}(\varphi) = \frac{m^*R_0^2}{4} \omega^2 (\varphi - \varphi_Q)^2,$$

respectively. A schematic plot of these two potentials is shown in Fig. 2(b). Once again we should solve the one-dimensional Schrödinger equation

$$\left\{ -\frac{\hbar^2}{2I} \frac{\partial^2}{\partial\varphi^2} + \frac{I\omega^2}{2}(\varphi - \varphi_Q)^2 - \varepsilon_j^{r.a.} \right\} \phi_j(\varphi - \varphi_Q) = 0,$$

where $I = m^*R_0^2/2$. It is nothing but an equation describing a shifted harmonic oscillator. The eigenfunctions and eigenvalues are thus given by

$$\phi_j(\varphi - \varphi_Q) = \frac{1}{\sqrt{2^j j!\, \pi^{1/2}\xi}} \exp\left[-\frac{1}{2}\left(\frac{\varphi - \varphi_Q}{\xi} \right)^2 \right]$$

$$\times H_j\left(\frac{\varphi - \varphi_Q}{\xi} \right),$$

$$\varepsilon_j^{r.a.} = \hbar\omega\left(j + \frac{1}{2} \right), \quad j = 0,1,2,\dots. \quad (24)$$

In Eq. (24), $\xi \equiv [(\hbar\omega/2)(\hbar^2/m^*R_0^2)]^{-1/2} \ll 1$ is the typical width of the single-well wave function and $H_j(x)$ is Hermite polynomial.[32] By substituting Eq. (21) in Eqs. (18) and (17), in the limit of small ξ, the final result is

$$t_{0,j} \approx \alpha_j \hbar \omega,$$

$$t_{1,j} \approx (-1)^j \beta_j \exp\left(-\frac{\pi^2}{\xi^2}\right) \hbar \omega,$$

and

$$\varepsilon_j^{r.a.,p} \approx \hbar \omega \left[\left(j+\frac{1}{2}\right) - \alpha_j + (-1)^{j+1} 2\beta_j \right.$$

$$\left. \times \exp\left(-\frac{\pi^2}{\xi^2}\right)\cos\left(\frac{2\pi\Phi}{\Phi_0}\right)\right],$$

where

$$\alpha_j = \frac{\xi^2}{24} \frac{1}{2^j j! \pi^{1/2}} \int_{-\infty}^{+\infty} dx\, x^4 H_j^2(x) \exp(-x^2),$$

$$\beta_j = \frac{(\pi^2-4)}{2^{j+1} j! \xi^2} H_j^2\left(\frac{\pi}{\xi}\right).$$

C. Coulomb interaction potential

Let us consider the more realistic Coulomb interaction potential which has the form [see also Fig. 2(c)]

$$V_{e\text{-}h}\left(2R_0\left|\sin\frac{\varphi}{2}\right|\right) = -\frac{e^2}{4\pi\varepsilon_0\varepsilon_r R_0 2|\sin(\varphi/2)|},$$

$$V_{e\text{-}h}^{SW,Q}(\varphi) = -\frac{e^2}{4\pi\varepsilon_0\varepsilon_r R_0 |\varphi-\varphi_Q|}.$$

We now face to solve the Schrödinger equation for a one-dimensional exciton,

$$\left\{-\frac{\hbar^2}{m^*R_0^2}\frac{\partial^2}{\partial\varphi^2} - \frac{e^2}{4\pi\varepsilon_0\varepsilon_r R_0|\varphi-\varphi_Q|} - \varepsilon_j^{r.a.}\right\}\phi_j(\varphi-\varphi_Q)$$

$$= 0.$$

The ground state solution gives a logarithmically divergent eigenvalue ($\varepsilon_j^{r.a.} \to -\infty$) and the normalized eigenfunction behaves like a δ function.[33] In this sense, the electron-hole pair tends to bind extremely tightly, and is prevented to tunnel through the Coulomb potential barrier to induce any measurable AB effect. This situation is also expected if one introduces a finite but small ring width W. On the other hand, each excited state of one-dimensional exciton is twofold degenerate and classified further by the *parity* symmetry parameter θ ($\theta=0$, and 1 corresponds to even and odd parity symmetry, respectively). The detailed eigenfunctions can be constructed from the radial wave function of a hydrogen atom with zero angular momentum and are given by

$$\phi_{j\theta}(\varphi-\varphi_Q) = \begin{cases} \psi_j(\varphi-\varphi_Q), & \varphi>\varphi_Q \\ (-1)^\theta \psi_j(\varphi-\varphi_Q), & \varphi<\varphi_Q \end{cases}, \quad j=1,2,\dots$$

$$\psi_j(\varphi-\varphi_Q) = \left(\frac{2}{j^3 a^3}\right)^{1/2} |\varphi-\varphi_Q| \exp\left(-\frac{|\varphi-\varphi_Q|}{ja}\right)$$

$$\times F\left(-j+1,2,\frac{2|\varphi-\varphi_Q|}{ja}\right),$$

where $a \equiv 2(\hbar^2/m^*R_0^2)/(e^2/4\pi\varepsilon_0\varepsilon_r R_0) \ll 1$ and F is a hypergeometric function.[32] The corresponding eigenvalues have the form

$$\varepsilon_{j\theta}^{r.a.} = -\frac{1}{aj^2}\frac{e^2}{8\pi\varepsilon_0\varepsilon_r R_0},$$

similar to the energy spectra of a hydrogen atom. It should be pointed out that the eigenfunctions vanish at $\varphi=\varphi_Q$ since the singular and nonintegrable Coulomb potential acts as an impenetrable barrier for both electron and hole.[34] This effect gives an exponentially small oscillator strength for the excited states [see Eq. (20)] and leads to the rapid damping of the low-lying excitonic transitions in the linear optical susceptibility for a finite width nanoring as shown in the next section. The hopping integrals in Eq. (18) are tedious to integrate, and in the first order of small-a limit the final answer is

$$t_{0,j} \approx \alpha_j \frac{e^2}{8\pi\varepsilon_0\varepsilon_r R_0},$$

$$t_{1,j} \approx (-1)^\theta \beta_j \exp\left(-\frac{2\pi}{ja}\right)\frac{e^2}{8\pi\varepsilon_0\varepsilon_r R_0},$$

and

$$\varepsilon_{j\theta}^{r.a.,p} \approx -\frac{e^2}{8\pi\varepsilon_0\varepsilon_r R_0}\left[\frac{1}{aj^2} + \alpha_j + (-1)^\theta 2\beta_j \right.$$

$$\left. \times \exp\left(-\frac{2\pi}{ja}\right)\cos\left(\frac{2\pi\Phi}{\Phi_0}\right)\right],$$

where

$$\alpha_j = \frac{ja}{48} \int_0^{+\infty} dx\, x^3 [F(-j+1,2,x)]^2 \exp(-x),$$

$$\beta_j = \frac{2\pi(\pi-2)}{j^3 a^3}(2\pi+ja)[F(-j+1,2,2\pi/ja)]^2.$$

At the end of this section, we would like to emphasize the following features.

(i) For all the cases we have considered, both for ground state and excited states the hopping integral $t_{1,j}$ is typically exponentially small compared with $\varepsilon_j^{r.a.}$, and the exponent factor is determined by the ratio of electron-hole interaction potential and the characteristic energy of rotation mode. This prediction is in apparent contradiction to the recent claim of

Römer and Raikh,[22] which predicted that the ABE oscillations are found much more easily in the case of excited states and are not exponentially small. This discrepancy might arise from the definition of ''excited states'' of excitons. Recall that there is only one bound state for an electron-hole pair with a short-ranged interaction potential (at least with a δ potential). Therefore, the ''excited states'' discussed by Römer and Raikh are more appropriately regarded as ''excited states'' of *free* electrons or holes instead of excitons.

(ii) In the case of the Coulomb interaction potential, there is no ABE for the ground excitonic state due to the intrinsic divergence of the ground state energy of one-dimensional excitons.[33]

(iii) On the other hand, in order to observe the AB effect in excited states, the single-well eigenvalues $\varepsilon_j^{r.a.}$ should be tuned closely to the potential maximum $V_{e\text{-}h}(\pi)$. Because of the particular properties of the energy spectra in the presence of Coulomb interaction, i.e., $\varepsilon_{j\theta}^{r.a.} \propto -1/j^2$, the Coulomb interaction potential is appropriate to observe the AB effect in excited states compared with other potentials. For example, for a narrow-width nanoring with $R_0 = 20$ nm, by setting $\varepsilon_{j\theta}^{r.a.} \sim -e^2/8\pi\varepsilon_0\varepsilon_r R_0$, a rough estimation gives $j \sim 1$, which agrees well with the numerical results for light-hole excitons in InAs nanorings as shown below.

IV. NUMERICAL RESULTS AND DISCUSSIONS

In order to understand the influence of a finite ring width on the AB effect, let us now discuss the numerical results for a *realistic* self-assembled semiconducting InAs nanoring. In the following we restrict ourselves in the subspace $L = 0$. We have taken the parameters $m_e^* = 0.067 m_e$, the effective mass of the light hole $m_{lh}^* = 0.099 m_e$, the effective mass of the heavy hole $m_{hh}^* = 0.335 m_e$ (m_e is the bare mass of a single electron), and $\varepsilon_r = 12.4$, which are appropriate for InAs material.[3,5,10] The electron and hole are considered to be confined in a confinement potential with the same strength, i.e., $m_e^* \omega_e^2 = m_h^* \omega_h^2$. The ring radius R_0 and characteristic frequency of the radial confinement $\hbar\omega_e$ are chosen to be 20 nm and 14 meV ($\hbar\omega_e = 14$ meV corresponds to $W = 10$ nm), respectively, simulating the recent experimental results $\Delta E_m \sim 5$ meV and $\Delta E_n \sim 20\text{-}25$ meV in InAs nanorings,[24] ΔE_m is the energy level spacing between the single electron states with different orbital angular momentum m and the same radial quantum number n, while ΔE_n corresponds to the energy spacing with different radial quantum number n and the same angular momentum m. In the calculations, we use effective atomic units in which the length unit a_B^* is a factor ε_r/μ times the Bohr radius a_B, and the energy is given in effective hartrees, $H_a^* = (\mu/\varepsilon_r^2) \times 1$ hartree (for the heavy-hole exciton, for example, the length and energy units then scale to $a_B^* = 11.8$ nm and $H_a^* = 10.0$ meV). For $R_0 = 20$ nm, the universal flux quantum Φ_0 corresponds to the magnetic field $B \approx 4.1$ T.

By probing of the structure of the numerical excitonic wave functions with the use of the conditional probability distribution (CPD) and pair-correlation function[35,36] (PCF),
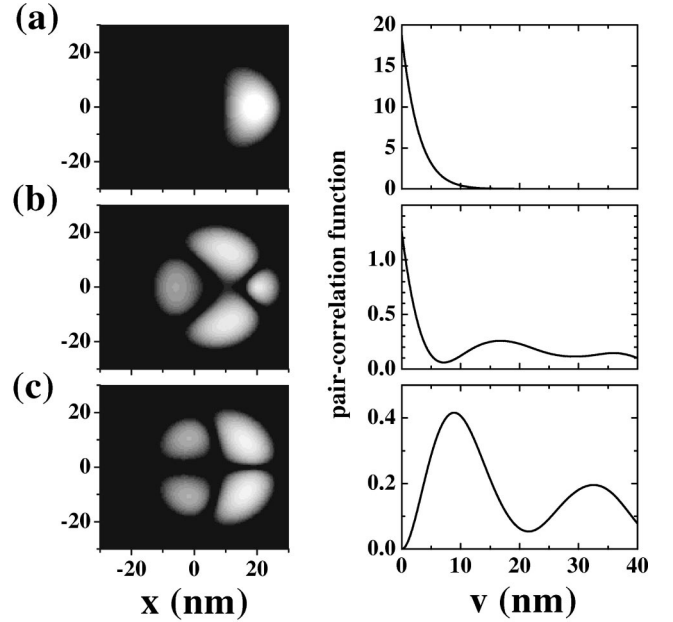

FIG. 3. The conditional probability distributions (CPD's) and pair-correlation functions (PCF's) shown, respectively, on the left and right of each of the subplots [labeled by (a)–(c)] for a heavy-hole exciton in an InAs nanoring with radius $R_0 = 20$ nm and width $W = 10$ nm. Each CPD is expressed in a logarithmic intensity scale in the range from 0.01 (black) to 1.0 (white). The heavy hole is fixed at $\mathbf{v}_0 = (20,0)$. (a) The ground state and (b) the fifth and (c) sixth excited states.

we first study the hopping integral $t_{1,j}$ (or the tunneling possibility) that plays the most essential role in the AB effect. Denoting the numerical wave function of excitons by $\Psi(\mathbf{r}_e, \mathbf{r}_h)$ [see Eq. (3), which is the summation of the product of the center-of-mass and relative wave functions], we define the usual PCF as

$$G(v) = 2\pi \int \int \delta(\mathbf{r}_e - \mathbf{r}_h - \mathbf{v}) |\Psi(\mathbf{r}_e, \mathbf{r}_h)|^2 d\mathbf{r}_e d\mathbf{r}_h, \tag{26}$$

and the CPD for finding the electron at $\mathbf{v}$ given that the hole is at $\mathbf{r}_h = \mathbf{v}_0$ as

$$\mathcal{P}(\mathbf{v}|\mathbf{r}_h = \mathbf{v}_0) = \frac{|\Psi(\mathbf{v}, \mathbf{r}_h = \mathbf{v}_0)|^2}{\int d\mathbf{r}_e |\Psi(\mathbf{r}_e, \mathbf{r}_h = \mathbf{v}_0)|^2}. \tag{27}$$

Note that for the exact Ψ in the case of a circularly symmetric confinement, the PCF turn out to be circularly symmetric.

With the above, we solved for heavy-hole–exciton energy spectra and wave functions for $W = 10$ nm. The selected PCF's and CPD's are displayed in Fig. 3. For the ground state in Fig. 3(a), the CPD exhibits a highly localized electron density around the hole, namely, the electron and hole tends to bind tightly with each other. The above picture is also reflected in the PCF, which shows a rapid delay as the distance between electron and hole increases. This behavior agrees well with the rigorous analysis presented earlier in Sec. III C. In contrast to the ground state, in Figs. 3(b) and
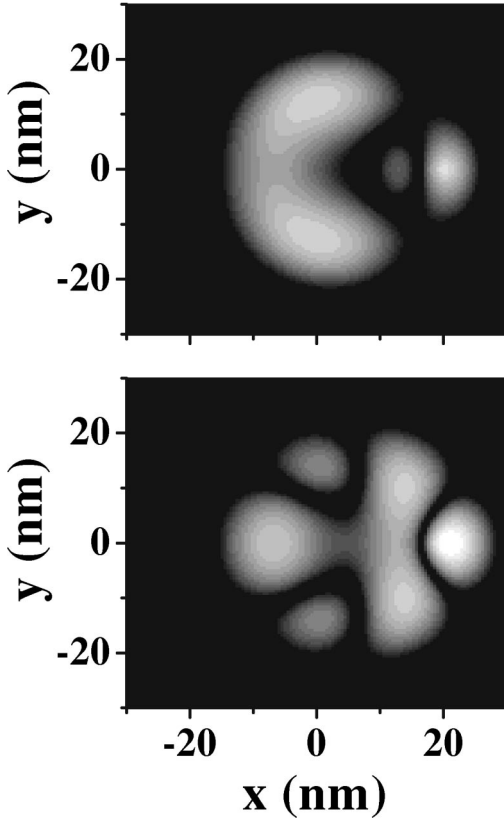
FIG. 4. The conditional probability distributions (CPD's) for the eighth (upper panel) and ninth (lower panel) excited states. Other parameters are the same as in Fig. 3.

FIG. 5. The low-lying energy levels of InAs nanorings with radius $R_0 = 20$ nm and width $W = 10$ nm as a function of the magnetic field for (a) heavy-hole and (b) light-hole excitons. As indicated by the arrow, a periodic, Aharonov-Bohm-type oscillation in some low-lying energy levels takes place.

This is due the comparable effective mass between the electron and light hole, which suppresses the electron-hole binding (i.e., the much higher ground-state energy of light-hole exciton compared with that of heavy-hole exciton) and thus enhances the AB effect.

Other noticeable features shown in Figs. 5(a) and 5(b) include the following. (i) There are many anticrossings in the energy levels that are caused by level repulsions. (ii) Contrary to conventional quantum dots, when the magnetic field is increased it seems unlikely to form any Landau levels. (iii) In the high magnetic field, the energy level of the ground state and first excited state shows a slight blueshift, due to the diamagnetic effect for each charge carrier that pushes all the relative energies upwards. This behavior is qualitatively similar to the excitons in quantum dots. Note that those blueshifts are observed in a recent experiment.[38]

The behavior of the oscillator strengths for heavy-hole exciton and light-hole exciton as a function of the magnetic field is presented in Figs. 6(a)–6(d). It is readily seen that periodic oscillations take place in the oscillator strengths for

3(c) the CPD's for the fifth and sixth excited states exhibit a well-developed local maximum probability for finding the electron around the diametrically opposite point $(-8,0)$, suggesting that the electron and hole have the possibility to tunnel through the Coulomb potential barrier in opposite directions. Observe also that the PCF's in Figs. 3(b) and 3(c) reveal a clear local maximum at $v \sim 35$ nm. Moreover, in the case of the eighth and ninth excited states (see Fig. 4), one can even identify a larger hopping integral. The remarkable emergence of the hopping integral for low-lying excited excitonic states provides us a possibility for observing a nonvanishing AB effect.

Figures 5(a) and 5(b) display the low-lying energy levels as a function of the magnetic field for heavy-hole exciton and light-hole exciton. As can be seen immediately, the most obvious feature is the AB oscillations of some low-lying energy levels (indicated by an arrow) with a period $B \approx 4.1$ T or a flux quantum Φ_0, as expected. However, the AB oscillations are not very close to sinusoidal as illustrated by Eq. (17), due to the finite width of nanorings. The typical amplitude of those oscillations is about 3 meV, which is much larger than the extremely narrow luminescence linewidth in a *single* InAs nanoring,[37] and in view of this it might be sensitive to be detected by present optical emission techniques. Comparing Figs. 5(a) and 5(b), it is seen that the energy levels of the light-hole exciton show a relatively pronounced AB effect. Even the first excited energy level of the light-hole exciton tends to oscillate with the magnetic field.
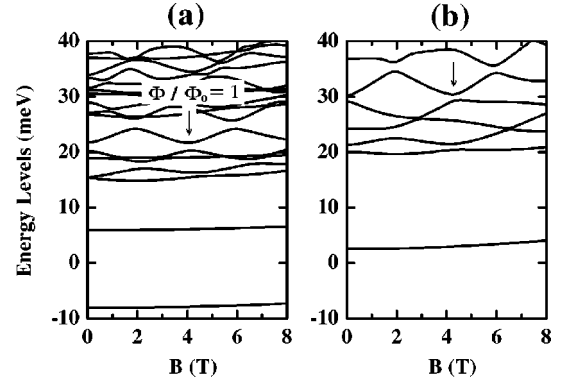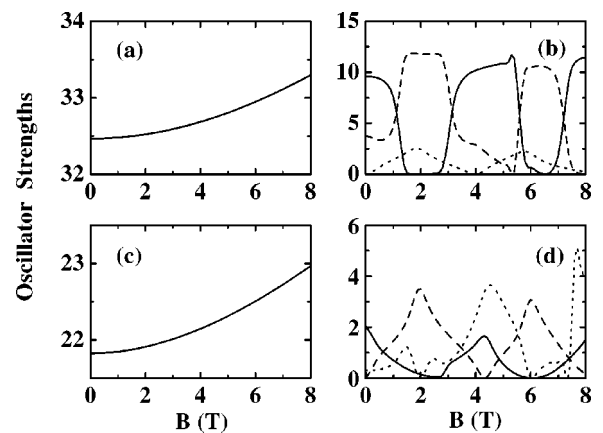

FIG. 6. The oscillator strengths of InAs nanorings as a function of the magnetic field for heavy-hole [upper panel, (a) and (b)] and light-hole [lower panel, (c) and (d)] excitons. (a),(c) for ground state and (b),(d) for excited states (the solid, dashed, and dotted lines correspond to the fourth, fifth, and sixth excited states).
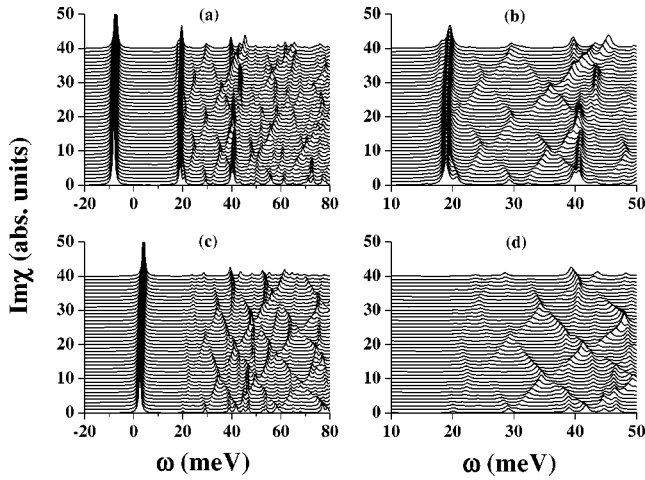
FIG. 7. Imaginary part of linear optical susceptibility as a function of frequency for different magnetic fields (in each subplot, from bottom to top, $B = 0.0$–8.0 T is increased on steps of 0.2 T). (a),(b) for heavy-hole and (c),(d) for light-hole excitons. (b) and (d) are the enlarged versions of (a) and (c). Ring radius $R_0 = 20$ nm and width $W = 10$ nm. For simplicity, the semiconducting band gap E_g is taken to be zero. Note that for the sake of clarity curves have been shifted up by a constant.

FIG. 8. The low-lying energy levels of InAs nanorings as a function of the magnetic field for a heavy-hole exciton with different ring widths: (a) $W = 8$ nm, (b) 14 nm, (c) 20 nm, and (d) 30 nm. Other parameters are the same as in Fig. 5.

the selected low-lying excited states. Though those oscillations are not regular in shape and not close to the expected sinusoidal, they are still supposed to be caused by AB phenomena. In contrast, for the ground state, the oscillator strength increase monotonically with the magnetic field. The result is in line with the blueshifts of the ground-state energies, for example, the increasing magnetic field increases the confinement, decreases the separation between electron and hole, and in turn yields the enhancement of oscillator strengths. Furthermore, the overall magnitude of the oscillator strength of the ground state is approximately one order larger that of low-lying excited states, in good agreement with the analysis presented earlier that the oscillator strengths for excited states are exponentially small for ideal one-dimensional nanorings.

To support the experimental relevance of our results and better understand the periodic, Aharonov-Bohm-type oscillation in energy spectra, the imaginary part of linear optical susceptibility is plotted as a function of frequency ω for different magnetic fields in Figs. 7(a)–7(d), where a broadening parameter $\Gamma = 0.5$ meV is used. Those curves represent all the possible transitions of excitonic states that would be measurable via photoluminescence excitation measurements (PLE). For simplicity, the semiconducting band gap E_g is taken to be zero, and the frequency ω at each transition (peak) corresponds to the energy level of excitons, for example, the negative ω at the lowest transition in Fig. 7(a) corresponds to the ground-state transition of heavy-hole exciton. As expected, the periodic oscillations at some low-lying energy levels ($\omega \sim 30$ meV) are well reflected. However, the amplitude of those oscillations is very small compared with that of the lowest transition because of the weak oscillator strengths of low-lying excited states. In fact, it is an indication of the delicate nature of the AB effect,
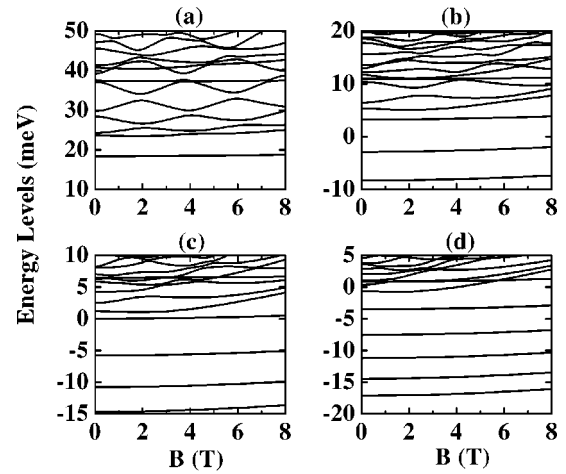
which suggests that a highly sensitive technique is needed in the experiment to access these coherent AB oscillations.

It is important to point out that our results mentioned above are in apparent contradiction with the prediction given by Song and Ulloa in their recent works, in which they claimed that the excitons in nanorings behave to a great extent as those in quantum dots of similar dimensions and the AB oscillation of exciton characteristics predicted for one-dimensional rings are found to not be present in finite-width systems.[23] Here we indeed observe the ABE of some of low-lying exciton states, which is suggested by the CPD's and PCF's, illustrated by the energy spectra and oscillator strengths and finally confirmed by the imaginary part of linear optical susceptibility. Therefore, we believe that the finite but small width of the nanorings will not suppress the ABE so greatly. Since the parameters used by Song and Ulloa are quite similar to ours, we suggest that the discrepancy might originate from the following reasons.

(i) In their paper, the negative Coulomb interaction term has been simply treated as a perturbation within a parabolic basis. However, just as the authors mentioned, when the characteristic scale of systems is beyond the effective Bohr radius, the known poor convergence of the parabolic basis might lead to unreliable results, especially for the excited states.

(ii) For the radius of the ring in Fig. 4 of Ref. 23, $R_0 = 24$ nm, the periodicity of the AB oscillation is expected to be given by a period $\Delta B \approx 2.9$ T. However, the authors only show the results for different magnetic fields increased in steps of 5.0 T. With such a large interval, one might miss the AB oscillations completely.

We next turn out to investigate the size effect by tuning the ring width. As an illustration, the low-lying energy levels of the heavy-hole exciton for a narrow ring width $W = 8$ nm, shown in Fig. 8(a), is compared to the wide ring width case with $W = 14$, 20, and 30 nm [shown in Figs. 8(b), 8(c), and 8(d), respectively]. It is readily seen that as the ring width increases, the AB oscillation pattern is gradually de-
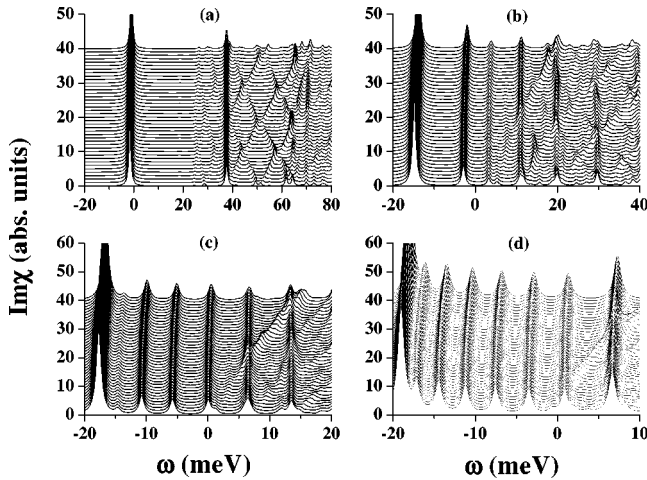
FIG. 9. Imaginary part of linear optical susceptibility of the heavy-hole exciton as a function of frequency for different magnetic fields and different ring widths: (a) $W = 8$ nm, (b) 14 nm, (c) 20 nm, and (d) 30 nm.

stroyed. The disappearance of the AB effect arises from the destruction of the non-simply-connected geometry of nanorings, since the increasing width lowers the soft confinement potential barrier at the ring center and in turn yields a high possibility for placement of carriers. For $W = 30$ nm, which is comparable to the ring diameter $d = 2R_0 = 40$ nm, the main characteristic of the energy spectra resembles that of quantum dots.[39–41] In Fig. 9, the corresponding imaginary part of linear optical susceptibility is plotted as a function of frequency. Comparison of the case of $W = 8$ nm in Fig. 9(a) with the wide width limit [Fig. 9(d)] is instructive, since it exhibits a distinctive difference of the excitonic optical properties between nanorings and quantum dots. Unlike conventional quantum dots, in which the low-lying exciton state transitions have the same amplitudes and are nearly equally distributed (a reflection of excitations involving the exciton ground state and various center-of-mass replicas without altering the ground state of the relative coordinate), the low-lying transitions of nanorings show a rapid dampening with frequency and their positions are not periodic. This difference is a refection of the anisotropic confinement of nanorings:[23] Since the exciton is confined in a quasi-one-dimensional system, its center-of-mass degree of freedom is greatly suppressed and its relative motion becomes dominant

(i.e., the general properties of a one-dimensional exciton is expected), thus resulting in the destruction of the regular patterns observed in quantum dots. It is interesting to note that this distinctive difference is indeed observed by a recent experiment given by Pettersson *et al.*[24] and Hu *et al.*[42,43]

V. CONCLUSION

In conclusion, we have studied the magnetic field effect on excitons in an InAs nanoring based on a simple model Hamiltonian. By numerical diagonalization, we calculate the low-lying energy levels, oscillator strengths, and the corresponding linear optical susceptibility. A periodic, Aharonov-Bohm-type oscillation is clearly revealed in some low-lying energy levels and linear optical susceptibility curves for a *realistic* self-assembled semiconducting InAs nanoring. This AB effect is well interpreted with the rigorous analysis for narrow-width nanorings.

In a recent work, Warburton *et al.* presented an experiment of optical emission in a *single* charge-tunable nanoring.[37] They studied the role of multiply charged exciton complexes with no applied magnetic field and found a shell structure in energy similar to that of quantum dots.[44,45] Therefore, encouraged by the rapidly developing nanotechniques for detection, i.e., the achievement of extremely narrow and temperature-insensitive luminescence lines from a single InAs nanoring in GaAs, we hope that our predictions of the ABE effects can be confronted in experiments in the future.

Note added. Recently, we communicated with the authors of Ref. 23. We were informed that the width of the ring used in their calculations (in Fig. 4 of Ref. 23) should have read 21 nm instead of the 8 nm that is mistakenly mentioned in the caption. Therefore, their results are not in contradiction with ours. In fact, their results in Fig. 4 are very similar to ours for the heavy-hole exciton with a ring width of 20 nm as shown in Fig. 9(c).

[1] A. Lorke and R. J. Luyken, Physica B **256**, 424 (1998).

[2] A. Lorke, R. J. Luyken, M. Fricke, J. P. Kotthaus, G. Medeiros-Ribeiro, J. M. Garcia, and P. M. Petroff, Microelectron. Eng. **47**, 95 (1999).

[3] A. Lorke, R. J. Luyken, A. O. Govorov, J. P. Kotthaus, J. M. Garcia, and P. M. Petroff, Phys. Rev. Lett. **84**, 2223 (2000).

[4] D. Mailly, C. Chapelier, and A. Benoit, Phys. Rev. Lett. **70**, 2020 (1993).

[5] A. Emperador, M. Pi, M. Barranco, and A. Lorke, Phys. Rev. B **62**, 4573 (2000).

[6] P. Borrmann and J. Harting, cond-mat/0008464 (unpublished).

[7] M. Koskinen, M. Manninen, B. Mottelson, and S. M. Reimann, cond-mat/0004095 (unpublished).

[8] A. Bruno-Alfonso and A. Latgé, Phys. Rev. B **61**, 15 887 (2000).

[9] X. S. Chen, Z.-Y. Deng, W. Lu, and S. C. Shen, Phys. Rev. B **61**, 2008 (2000).

[10] H. Hu, J.-L. Zhu, and J. J. Xiong, Phys. Rev. B **62**, 16 777 (2000).

[11] J. Yi, H. Doh and S.-I. Lee, Phys. Rev. B **59**, 12 192 (1999).

[12] E. Ben-Jacob, F. Guinea, Z. Hermon, and A. Shnirman, Phys. Rev. B **57**, 6612 (1998).

[13] C. A. Stafford and D. F. Wang, Phys. Rev. B **56**, R4383 (1997).

[14] L. Wendler and V. M. Fomin, Phys. Rev. B **51**, 17 814 (1995).

[15] L. Wendler, V. M. Fomin, A. V. Chaplik, and A. O. Govorov, Phys. Rev. B **54**, 4794 (1996).

[16] L. Wendler, V. M. Fomin, A. V. Chaplik, and A. O. Govorov, Z. Phys. B: Condens. Matter **102**, 211 (1996).

[17] T. Chakraborty and P. Pietiläinen, Phys. Rev. B **50**, 8460 (1994).

[18] V. Gudmundsson and Á. Loftsdóttir, Phys. Rev. B **50**, 17 433 (1994).

[19] V. Halonen, P. Pietiläinen, and T. Chakraborty, Europhys. Lett. **33**, 377 (1996).

[20] K. Niemelä, P. Pietiläinen, and P. Hyvönen, and T. Chakraborty, Europhys. Lett. **36**, 533 (1996).

[21] A. Chaplik, Pis'ma Zh. Éksp. Teor. Fiz. **62**, 885 (1995) [JETP Lett. **62**, 900 (1995)].

[22] R. A. Römer and M. E. Raikh, Phys. Rev. B **62**, 7045 (2000).

[23] J. Song and S. E. Ulloa, Phys. Rev. B **63**, 125302 (2001).

[24] H. Pettersson, R. J. Warburton, A. Lorke, K. Karrai, J. P. Kotthaus, J. M. Garcia, and P. M. Petroff, Physica E (Amsterdam) **6**, 510 (2000).

[25] H. Hu, J.-L. Zhu, and J.-J. Xiong (unpublished).

[26] J.-L. Zhu, J. J. Xiong, and B.-L. Gu, Phys. Rev. B **41**, 6001 (1990).

[27] J.-L. Zhu, Z. Q. Li, J. Z. Yu, K. Ohno, and Y. Kawazoe, Phys. Rev. B **55**, 1 (1997).

[28] J. Song and S. E. Ulloa, Phys. Rev. B **52**, 9015 (1995).

[29] G. W. Bryant, Phys. Rev. B **37**, 8763 (1988).

[30] W. Que, Phys. Rev. B **45**, 11 036 (1992).

[31] Recently, we obtained Ref. 21, in which the main result is similar to that in Sec. III C.

[32] M. Abramowitz and I. A. Stegun, *Handbook of Mathematical Functions* (Dover, New York, 1972).

[33] R. Loudon, Am. J. Phys. **27**, 649 (1959).

[34] M. Andrews, Am. J. Phys. **44**, 1064 (1976).

[35] C. Yannouleas and U. Landman, Phys. Rev. B **61**, 15 895 (2000).

[36] C. Yannouleas and U. Landman, Phys. Rev. Lett. **85**, 1726 (2000).

[37] R. J. Warburton, C. Schäflein, D. Haft, F. Bickel, A. Lorke, K. Karrai, J. M. Garcia, W. Schoenfeld, and P. M. Petroff, Nature (London) **405**, 926 (2000).

[38] H. Pettersson (private communication).

[39] V. Halonen, T. Chakraborty, and P. Pietiläinen, Phys. Rev. B **45**, 5980 (1992).

[40] A. Wojs and P. Hawrylak, Phys. Rev. B **51**, 10 880 (1995).

[41] P. Hawrylak, Phys. Rev. B **60**, 5597 (1999).

[42] H. Hu, G.-M. Zhang, J.-L. Zhu, and J. J. Xiong, Phys. Rev. B **63**, 045320 (2001).

[43] H. Hu, D. J. Li, J.-L. Zhu, and J. J. Xiong, J. Phys.: Condens. Matter **12**, 9145 (2000).

[44] M. Bayer, O. Stern, P. Hawrylak, S. Fafard, and A. Forchel, Nature (London) **405**, 923 (2000).

[45] P. Hawrylak, G. A. Narvaez, M. Bayer, and A. Forchel, Phys. Rev. Lett. **85**, 389 (2000).